NANO LETTERS

2007
Vol. 7, No. 4
1095−1099

Hyperbranched Lead Selenide Nanowire Networks

Jia Zhu,[†] Hailin Peng,[‡] Candace K. Chan,[§] Konrad Jarausch,[||] Xiao Feng Zhang,[||] and Yi Cui*[,‡]

Department of Electrical Engineering, Department of Materials Science and Engineering, and Department of Chemistry, Stanford University, Stanford, California 94305, and Electron Microscope Division, Hitachi High Technologies America, Inc., 5100 Franklin Drive, Pleasanton, California 94588

Received January 7, 2007; Revised Manuscript Received February 27, 2007

ABSTRACT

Lead chalcogenide nanostructures are good potential candidates for applications in multiexciton solar cells, infrared photodetectors, and electroluminescence devices. Here we report the synthesis and electrical measurements of hyperbranched PbSe nanowire networks. Hyperbranched PbSe nanowire networks are synthesized via a vapor–liquid–solid (VLS) mechanism. The branching is induced by continuously feeding the PbSe reactant with the vapor of a low-melting-point metal catalyst including In, Ga, and Bi. The branches show very regular orientation relationships: either perpendicular or parallel to each other. The diameter of the individual NWs depends on the size of the catalyst droplets, which can be controlled by the catalyst vapor pressure. Significantly, the hyperbranched networks can be grown epitaxially on NaCl, a low-cost substrate for future device array applications. Electrical measurements across branched NWs show the evolution of charge carrier transport with distance and degree of branching.

Lead chalcogenides (PbE, E = S, Se, Te) are a special class of IV−VI narrow-band-gap (0.2−0.4 eV) semiconductors. Quantum confinement of charge carriers in PbE can be much stronger than in most II−VI and III−V semiconductors.[1] The energy level spacing can be even larger than the bulk band gap. The similar and small effective masses of both the electrons and the holes imply that this strong confinement effect is split equally between electrons and holes so that the electronic structure is simple. Quantum-confined PbE nanocrystals[1−4] have been exploited for transistors,[2] multiexciton generation,[5,6] polymer-composite infrared photodetectors,[7] and electroluminescence devices.[8]

Applications in these areas require good charge transport over long distances, which is more efficient in extended nanowire (NW) and branched NW structures than in spherical nanocrystals. PbE NWs have been synthesized by a variety of methods including chemical vapor transport (CVT),[9] mesoporous templating,[10] seeded solution approach (SSA),[11] oriented attachment of nanocrytals (OAN),[12] and colloidal synthesis.[13] Among them, CVT, SSA, and OAN methods have produced branched NW structures. For example, Ge et. al.[9] used $PbCl_2$ and Se as CVT precursors to produce PbS NWs. NWs grow epitaxially out of PbS crystalline seeds, forming only one generation of branched structures via a surface-defect-assisted mechanism. Here we exploit the vapor−liquid−solid (VLS) mechanism for hyperbranched NWs.[14−23] Multigenerations of PbSe NW branches are induced by continuously feeding the reactant with low-melting metal catalysts such as In, Ga, or Bi. The branches within a hyperbranched network show unprecedented regular order compared to previous studies. The hyperbranched networks can be grown epitaxially on NaCl substrates, a low-cost substrate for future device array applications. In situ electrical measurements across branched NWs reveal the evolution of charge carrier transport with distance and degree of branching.

The synthesis of hyperbranched PbSe NW networks was first realized by coevaporation of PbSe with a small amount of In_2Se_3 powder in a tube furnace, similar to our previous studies.[24−27] NWs were grown on Si ⟨001⟩ substrates with a native oxide or on NaCl ⟨001⟩ substrates. The substrates were placed downstream in a 1 in. diameter horizontal tube furnace (Lindberg/Blue M) with the source material, PbSe (Sigma Aldrich, Purity 99.999%) and In_2Se_3 (Sigma Aldrich, Purity 99%) placed in the hot center region. A 5% H_2 in N_2 gas mixture acted as a carrier gas to transport the vapor to the colder furnace region. Before each experiment, the quartz tube of the furnace was evacuated to <100 mTorr and flushed with the carrier gas repeatedly to decrease oxygen

* To whom correspondence should be addressed. E-mail: yicui@stanford.edu.
[†] Department of Electrical Engineering, Stanford University.
[‡] Department of Materials Science and Engineering, Stanford University.
[§] Department of Chemistry, Stanford University.
[||] Hitachi High Technologies America, Inc.

10.1021/nl0700393 CCC: $37.00
Published on Web 03/10/2007

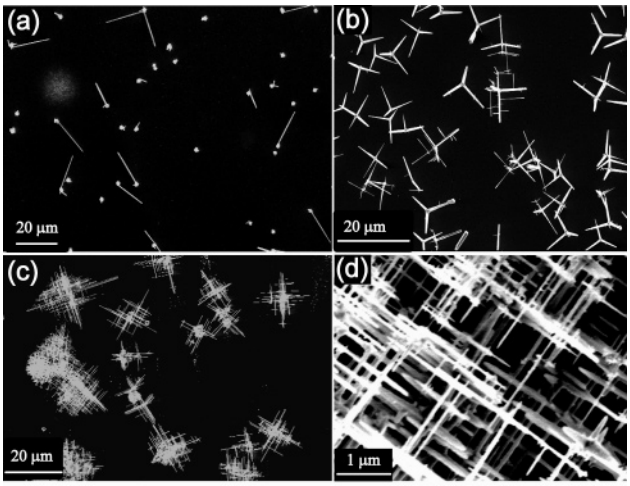

Figure 1. SEM images of PbSe NW network on Si ⟨100⟩ substrate grown for (a) 5 min, (b) 10 min, (c) 30 min; (d) high-resolution SEM image of PbSe NW network from (c).

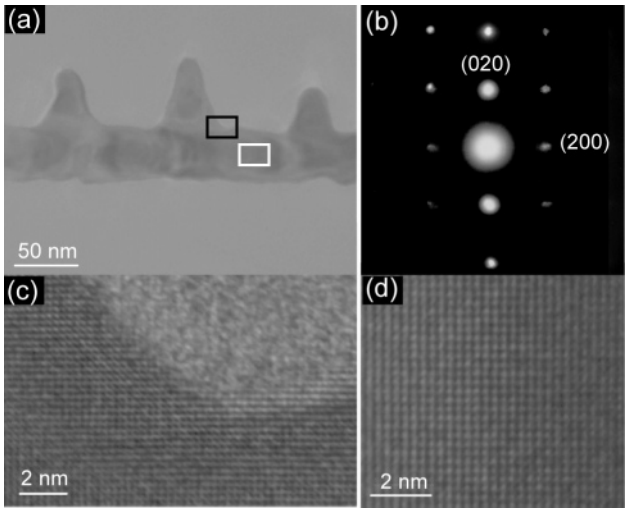

Figure 2. (a) TEM image of a branched PbSe NW. (b−c) SAD pattern and HRTEM image of the PbSe NW obtained at the branching interface (black rectangle in (a)), respectively. (d) HRTEM image of the main PbSe NW (white rectangle in (b)).

contamination. The typical synthesis conditions are: 0.2 g PbSe and 0.01 g In_2Se_3, pressure = 1 atm and temperature = 600−700 °C, duration time = 5−30 min, and carrier gas flow rate = 150 sccm. PbSe NW networks grew preferentially at the position of 10 cm away from the hot center region of the furnace, where the temperature was ∼400 °C. The NW surface morphologies were examined in an FEI Sirion scanning electron microscope (SEM). Samples were also transferred onto carbon film supported by copper grids for studies with a Philips CM20 transmission electron microscope (TEM) and energy dispersive X-ray spectrometry (EDX). The electrical properties were measured using a Hitachi N-6000 Nanoprober composed of six precisely position-controlled probes and a high-resolution field emission gun SEM.

Figure 1 shows the SEM images of as-grown products on a ⟨001⟩ Si substrate surface with intrinsic oxide at different times and indicates the formation process of the hyperbranched NW networks. At the initial stage of growth (5 min, Figure 1a), some NWs have reached lengths of 10−20 μm while others have just nucleated. At 10 min (Figure 1b), there are no visible particles as at 5 min, suggesting that all the particles have nucleated NWs. Each nanostructure shows at least one generation of branching, i.e., three NW branches, and some have a couple of generations of branching resulting in a hierarchical structure. At 30 min, NWs show many generations of branching, resulting in the hyperbranched NW networks. The number of branching generations reported here is significantly more than in previous studies.[14−23] There are several key characteristics that can be identified from SEM studies: first, the diameters of most NW branches are ∼100 nm and do not change significantly over the course of the growth process. Second, the maximum length of each NW branch is limited to ∼10−20 μm and does not increase significantly with the growth process. Third, the branches within the same NW network show a preferred orientation and appear to be perpendicular or parallel to each other, implying crystallographic registry.

The composition and structure of NW networks are studied using EDX and TEM. The EDX data (Figure S1 in Supporting Information) show that NW networks consist of Pb and Se with an atomic ratio of ∼1:1. Figure 2a shows a TEM image of a NW with three branches just nucleated. The directions of the main and branched NWs form a 90° angle, consistent with SEM observation. The high-resolution TEM (HRTEM) images taken on the main NW (Figure 2d) show that it is single-crystalline, and the spacing of the lattice planes parallel or perpendicular to the NW long axis is 3.06 Å, consistent with the (200) planes of the PbSe rock-salt structure. HRTEM at the branching interface (Figure 2c) gives the same lattice spacing and shows the single-crystalline nature of branches extending from the main NW. These data suggest that the main and branched NWs belong to the same single crystal. The single-crystalline nature of the whole NW network is further confirmed by selected-area electron diffraction (SAD) taken at the interface of main and branched NWs (Figure 2b). The SAD shows a square lattice, which can be indexed as the diffraction patterns along the ⟨001⟩ zone axis. The long axis of the main and branched NWs is along the same crystallographic direction of ⟨100⟩, consistent with HRTEM studies. A finding from EDX and HRTEM studies is that our NWs grown from PbSe precursors do not have a SiO_2 coating as in the NWs made previously by $PbCl_2$ and chalcogen CVT method.[9] This finding is important for future NW device processing.

We believe that the formation of hyperbranched NW networks is through a metal-catalyzed VLS mechanism. The participation of In_2Se_3 during growth is necessary for growing NWs and inducing branching. The growth without In_2Se_3 does not produce NWs but only gives large-size PbSe crystals (Figure S2 in Supporting Information). Indium vapor from the evaporation of In_2Se_3 may condense to form a nanoscale liquid droplet for PbSe NW nucleation and growth due to the low melting temperature of In. The existing In vapor in the subsequent growth process continuously supplies nanocatalysts onto the preformed NWs to nucleate and grow the

new branches. If this conjecture is true, we should be able to produce PbSe branched NWs with In metal precursors. Indeed, by placing In powder upstream at the temperature ~400 °C during PbSe vapor transport, we are able to produce branched NWs (Figure 3a) with morphology similar as using In_2Se_3 powder. Interestingly, other high-vapor-pressure metals such as Ga and Bi metals can also function as efficient catalysts for PbSe hyperbranched NWs (Figure 3b and c, respectively). It is challenging to predict the VLS growth conditions from the complex ternary phase diagrams in Pb−Se and −In, −Ga, or −Bi, although it seems generally true that these low-melting-point metals can function as good VLS catalysts or solvents to dissolve the PbSe vapor and nucleate and grow PbSe NWs.

An important phenomenon in VLS growth is the appearance of metal catalyst particles at the tips of NWs. However, the majority of the PbSe NW branches usually show a tapered shape at the tip (Figure 2a) without the presence of metal catalyst. We think that the absence of catalyst nanoparticles on most branches after synthesis might be due to the shrinkage and disappearance of catalysts through evaporation because they have a high vapor pressure. Another possible mechanism is through diffusion, which has recently been suggested in tapered Si NW grown using Au nanoparticles as catalysts.[28,29] However, some NW branches do preserve their catalysts at the tip. Figure 3d shows a TEM image of a Bi particle at the tip of a PbSe branch. Under the 200 keV electron beam, the Bi particle disappears within 30 s and leaves behind only the PbSe NW branch (Figure 3e). The observation is consistent with the volatility of low-melting-point metal catalysts and confirms the VLS growth mechanism.

The metal catalyst should be preserved if the collecting substrate temperature is lowered. To study this temperature effect, we also collected the synthesis product at the furnace's downstream edge, where the temperature is only 200 °C. SEM images on as-grown samples show that high-density NWs are grown and each has a catalyst particle clearly seen at the tip, although there is no regular branched NW formation (Figure 3f). Branched NWs are not observed at low temperatures because branching involves new nucleation events, which require some activation energy. Insufficient thermal energy is available at the lower temperature to overcome this activation barrier. However, low-temperature growth does preserve the catalyst particles. This observation provides further important evidence that the growth of PbSe NWs and their branches is via a VLS mechanism.

In the VLS mechanism, the catalyst size control can be used to control the size of hyperbranched NWs. Figure 4 a and b show the In metal-source-catalyzed PbSe NWs obtained from different furnace set temperature. It is shown clearly that decreasing the temperature from 700 to 650 °C will cause the reduction of the diameter of NWs from 150 to 100 nm. In fact, decreasing the set temperature is expected to decrease the In vapor pressure as well as the In−PbSe alloy particle size. Alternatively, the furnace temperature can remain unchanged while the temperature of the metal powder is changed by placing it at a different location in the tube

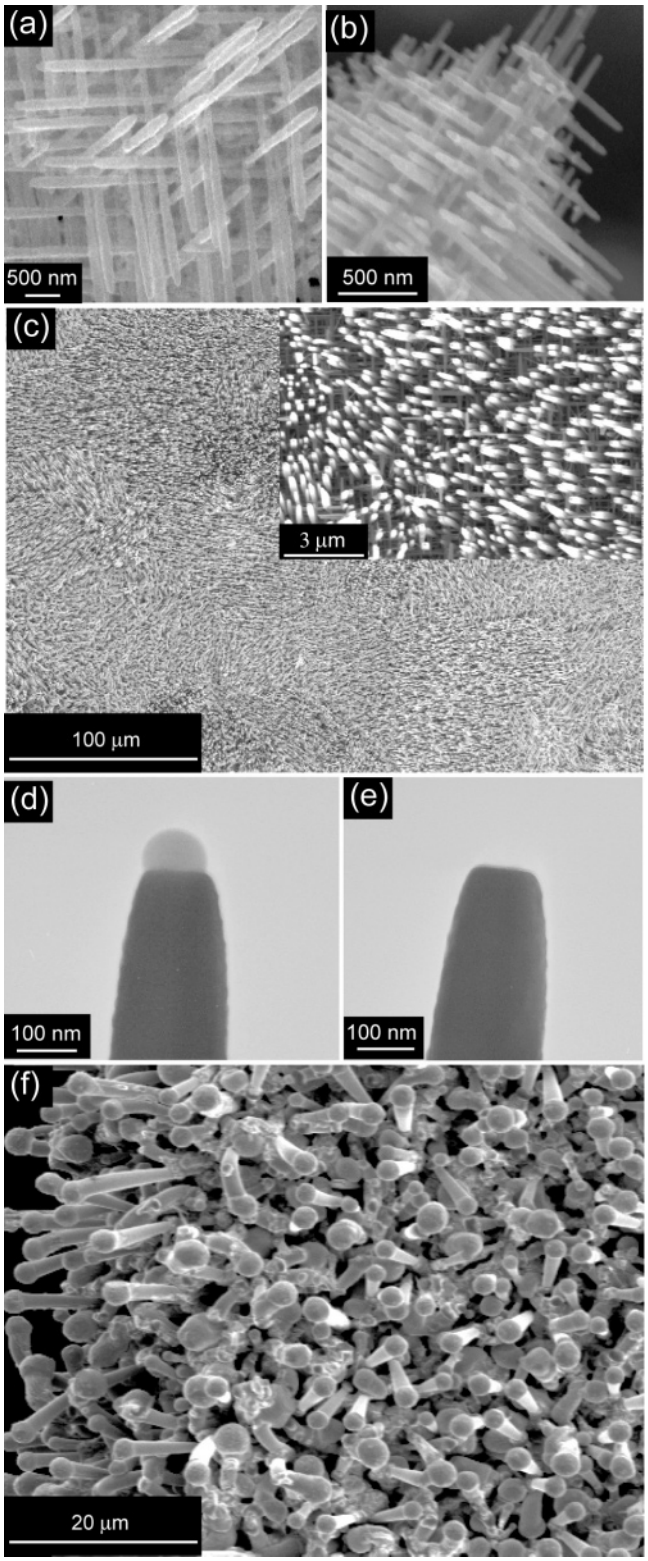

Figure 3. (a−b) SEM images of PbSe NWs using indium, gallium as catalyst, growth for 60 min; (c) SEM image of PbSe NWs using bismuth as catalyst, growth for 120 min, inset is a zoomed in picture; (d−e) TEM image of PbSe NWs with and without Bi particles; (f) SEM image of PbSe NWs with Bi particles at the end.

furnace. For example, Figure 4c and d shows that the In powder was placed at locations with temperatures of 350 and 400 °C, respectively. The lower temperature resulted in

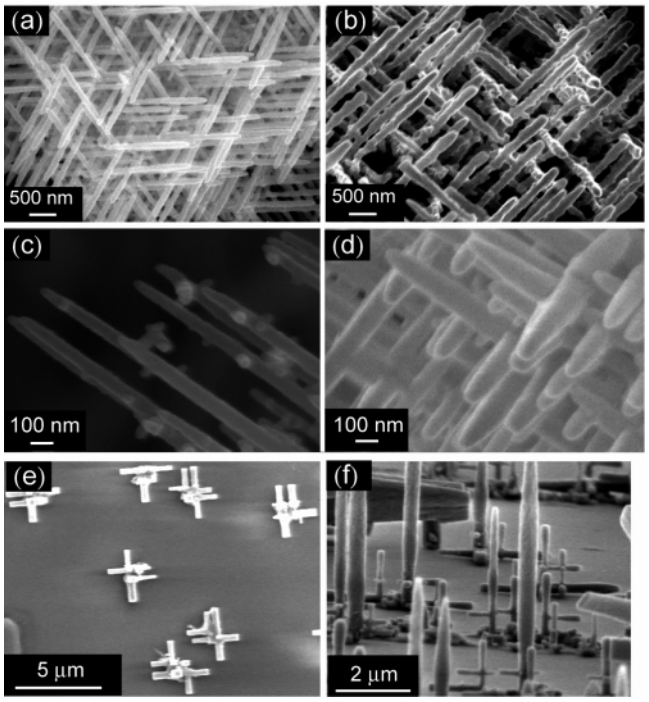

Figure 4. (a−b) SEM images of PbSe NWs with different growth temperature: 650 and 700 °C, respectively, (c−d) SEM images of PbSe NWs with different indium temperature: 350 and 400 °C, respectively, (e−f) top-view and cross-section SEM images of epitaxial growth of PbSe NWs on NaCl ⟨001⟩ substrate.

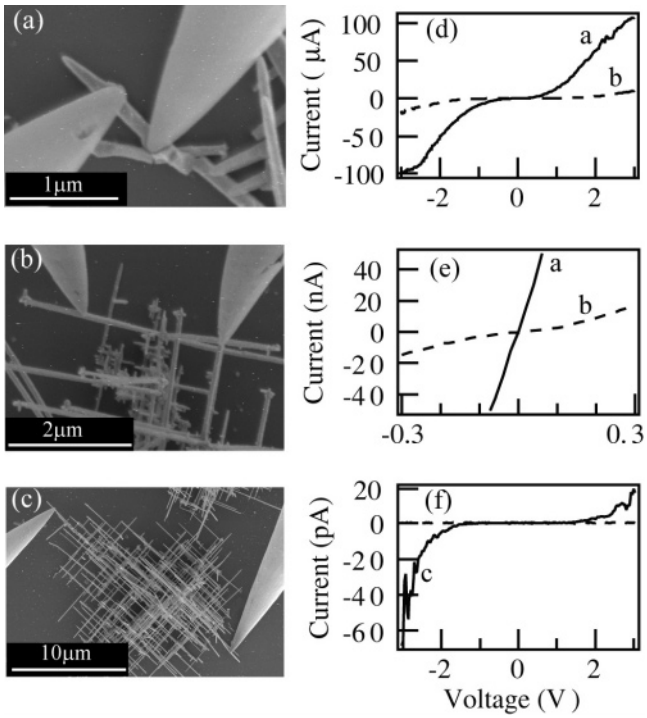

Figure 5. (a−c) SEM images of hyperbranched NW networks contacted by two tungsten probes. (d) $I-V$ data with curve a and b corresponding to the cases in (a) and (b), respectively. (e) is the low bias region of (d). The solid line in (f) is the $I-V$ data for (c), and the dashed line is the $I-V$ data through the substrate.

thinner NWs (∼60 nm) than the higher temperature NWs (∼100 nm).

PbSe hyperbranched NW networks grown on Si substrates with intrinsic amorphous oxide do not show orientation registry between different networks (Figure 1c). Because the capability of orientation control is important for device applications, we studied the orientation control by using the concept of NW epitaxial growth on a crystalline substrate surface. PbSe has a rock-salt structure with a lattice parameter of 6.124 Å. We choose a NaCl ⟨001⟩ substrate, which has a lattice parameter of 5.65 Å. Despite the large lattice mismatch of 8.4%, PbSe NW networks can still be epitaxially grown onto the NaCl substrate. Top-view SEM images as that in Figure 4e show that all the NW branches in different networks orient only in two perpendicular directions, suggesting that NW networks have a perfect registry with respect to each other. These two preferred directions are parallel to the NaCl [100] and [010] directions, respectively. Side-view SEM images (Figure 4f) taken by tilting the substrate indicate that the third orientation is perpendicular to the substrate surface, i.e., along the [001] direction, consistent with the growth direction of PbSe NWs. We emphasize the significance of using NaCl substrates for orientation control because NaCl is a low-cost substrate for device fabrication.

To study the electrical properties of these hyperbranched PbSe NW networks, we have carried out electron transport measurements on a single network. Because the branches extend out three-dimensionally to tens of micrometers, it is challenging to pattern the metal contact electrodes by lithography methods. Here we exploit in situ nanoscale tungsten probes as contact electrodes in a Hitachi N-6000 Nanoprober instrument. The probe tips have sizes below 100 nm, which is comparable to the size of the NWs, and the probe positions are controlled by piezoelectric actuators with a nanometer precision. Right before contacting the NWs, the probes were shorted (<100 Ω resistance) to ensure that the tungsten oxide layer on the probe surface is thin enough. The leakage current through the substrate was immeasurably small (the dashed curve in Figure 5f). The contact formation betweens probes and NWs can be monitored with in situ SEM before, during, and after electrical measurements. Part a−c of Figure 5 are the SEM images showing the three cases: first, single NW branch is contacted (Figure 5a); second, a junction locates between the two probes, i.e., two NW branches are contacted (Figure 5b); third, electrons transport through many junctions or NW branches (Figure 5c). In the first case, current (I) measured against voltage (V) (Figure 5d, curve a) shows nonlinear characteristics with resistance ∼1 MΩ at low (Figure 5e, curve a) and ∼40 kΩ at high voltage, suggesting there are energy barriers along the transport pathway. In the second case, $I-V$ curves (Figure 5d and e, curve b) indicate that the resistance increases significantly to 30 MΩ at low and ∼400 kΩ at high voltage. In the third case, the resistance increases to very high values: ∼10 TΩ at low and 5 GΩ at high bias. Careful data analysis indicates the following important facts: (1) Resistance at low bias increases with the length of electron transport pathway much faster than at high bias. By a rough estimation, the resistance at high bias increases linearly with the pathway length. (2) The high resistance region at low bias is widened with the pathway length increase, suggesting

that the energy barrier also increases. This energy barrier may have a contribution from the metal probe−NW contact and from the branched NW themselves because of the mechanical bending of NWs forced by metal probes and the multiple intra-NW p-n junction formation. It is well-known that PbSe can be p- or n-type, depending on the stoichiometry.[30] The variation of stoichiometry (Figure S1 in Supporting Information) in the large branched NW networks can cause the formation of many p-n junctions. These possible explanations require future study.

In conclusion, we have successfully synthesized PbSe hyperbranched NW networks via a VLS mechanism. Low-melting-point metals such as In, Ga, or Bi can function as VLS catalysts. The NW networks exhibit regular 90° branching, consistent with the crystalline orientation of the rock-salt structure. The diameter of the individual NWs can be controlled. The hyperbranched NW networks can be grown epitaxially on NaCl substrate, which is a low-cost substrate for future device array applications. Electrical measurements across branched NWs indicate the evolution of charge carrier transport with distance and degree of branching. The hyperbranched lead chalcogenide NW networks might serve as promising candidates for multiexciton solar cells, photodetectors, and light emission devices.

Acknowledgment. We thank Prof. McGehee and Prof. Nix for helpful discussion. Y.C. acknowledges support from Stanford New Faculty Startup Fund and CPN seed fund. J.Z. acknowledges support from a CPN Fellowship. C.K.C. acknowledges support from a NSF Graduate Fellowship and Stanford Graduate Fellowship.

Supporting Information Available: EDX data of PbSe NW network, SEM of product without In_2Se_3 source. This material is available free of charge via the Internet at http://pubs.acs.org.

References

(1) Wise, F. W. *Acc. Chem. Res.* **2000**, *33*, 773.
(2) Talapin, D. V.; Murray, C. B. *Science* **2005**, *310*, 86.
(3) Du, H.; Chen, C.; Krishnan, R.; Kraus, T. D.; Harbold, J. M.; Wise, F. W.; Thomas, M. G.; Silcox, J. *Nano Lett.* **2002**, *2*, 1321.
(4) Wehrenberg, B. L.; Wang, C.; Guyot-Sionnest, P. *J. Phys. Chem. B* **2002**, *106*, 10634.
(5) Schaller, R. D.; Klimov, V. I. *Phys. Rev. Lett.* **2004**, *92*, 186601.
(6) Ellingson, R.; Beard, M. C.; Johnson, J. C.; Yu, P.; Micic, O. I.; Nozik, A. J.; Shabaev, A.; Efros, A. L. *Nano Lett.* **2005**, *5*, 865.
(7) McDonald, S. A.; Konstantatos, G.; Zhang, S.; Cyr, P. W.; Klem, E. J. D.; Levina, L.; Sargent, E. H. *Nat. Mater.* **2005**, *4*, 138.
(8) Steckel, J. S.; Coe-Sullivan, S.; Bulovic, V.; Bawendi, M. *Adv. Mater.* **2003**, *15*, 1862.
(9) Ge, J.-P.; Wang, J.; Zhang, H.-X.; Wang, X.; Peng, Q.; Li, Y. D *Chem.−Eur. J.* **2005**, *11*, 1889.
(10) Gao, F.; Lu, Q.; Liu, X.; Yan, Y.; Zhao, D. *Nano Lett.* **2001**, *1*, 743.
(11) Hull, K. L.; Grebinski, J. W.; Kosel, T. H.; Kuno, M. *Chem. Mater.* **2005**, *17*, 4416.
(12) Cho, K.-S.; Talapin, D. V.; Gashler, W.; Murray, C. B. *J. Am. Chem. Soc.* **2005**, *127*, 7140.
(13) Lifshitz, E.; Bashouti, M.; Kloper, V.; Kigel, A.; Eisen, M. S.; Berger, S. *Nano Lett.* **2003**, *3*, 857.
(14) Gao, P.; Wang, Z. L. *J. Phys. Chem. B* **2002**, *106*, 12653.
(15) Yan, H.; He, R.; Johnson, J.; Law, M.; Saykally, R. J.; Yang, P. *J. Am. Chem. Soc.* **2003**, *125*, 4728.
(16) Lao, J. Y.; Wen, J. G.; Ren. Z. F. *Nano Lett.* **2002**, *2*, 1287.
(17) Wang, D.; Qian, F.; Yang, C.; Zhong, Z.; Lieber, C. M. *Nano Lett.* **2004**, *4*, 871.
(18) May, S. J.; Zheng, J.; Wessels, B. W.; Lauhon, L. J. *Adv. Mater.* **2005**, *17*, 598.
(19) Dick, K. A.; Deppert, K.; Karlsson, L. S.; Seifert, W.; Wallenberg, L. R.; Samuelson, L. *Nano Lett.* **2006**, *6*, 2842.
(20) Jung, Y.; Ko, D.-K.; Agarwal, R. *Nano Lett.* **2007**, *7*, 264.
(21) Yang, R.; Chueh, Y.; Mober, J. R.; Snyder, R.; Chou, L.; Wang, Z. L. *Nano Lett.* **2007**, *7*, 269.
(22) Zhou, J.; Ding, Y.; Deng, S. Z.; Gong, L.; Xu, N. S.; Wang, Z. L. *Adv. Mater.* **2005**, *17*, 2107.
(23) Ponzoni, A.; Comini, E.; Sberveglieri, G.; Zhou, J.; Deng, S. Z.; Xu, N. S.; Ding, Y.; Wang, Z. L. *Appl. Phys. Letts.* **2006**, *88*, 203101.
(24) Meister, S.; Peng, H.; McIlwrath, K.; Jarausch, K.; Zhang, X. F.; Cui, Y. *Nano Lett.* **2006**, *6*, 1514.
(25) Peng, H.; Meister, S.; Chan, C. K.; Zhang, X. F.; Cui, Y. *Nano Lett.* **2007**, *7*, 199.
(26) Peng, H.; Schoen, D. T.; Meister, S.; Zhang, X. F.; Cui, Y. *J. Am. Chem. Soc.* **2007**, *129*, 34.
(27) Chan, C. K.; Peng, H.; Twesten, R. D.; Jarausch, K.; Zhang, X. F.; Cui, Y. *Nano Lett.* **2007**, *7*, 490.
(28) Hannon, J. B.; Kodambaka, S.; Ross, F. M.; Tromp, R. M. *Nature* **2006**, *440*, 69.
(29) Cao, L.; Garipcan, B.; Atchison, J. S.;, Ni, C.; Nabet, B.; Spanier, J. E. *Nano Lett.* **2006**, *6*, 1852.
(30) Abrikosov, N. Kh.; Bankina, V. F.; Poretskaya, L. V.; Shelimova, L. E.; Skudnova, E. V. *Semiconducting II-VI, IV-VI, and V-VI Compounds*; Plenum Press, New York, **1969**; pp 82−90.

NL0700393